Published OnlineFirst November 20, 2013; DOI: 10.1158/1541-7786.MCR-13-0336

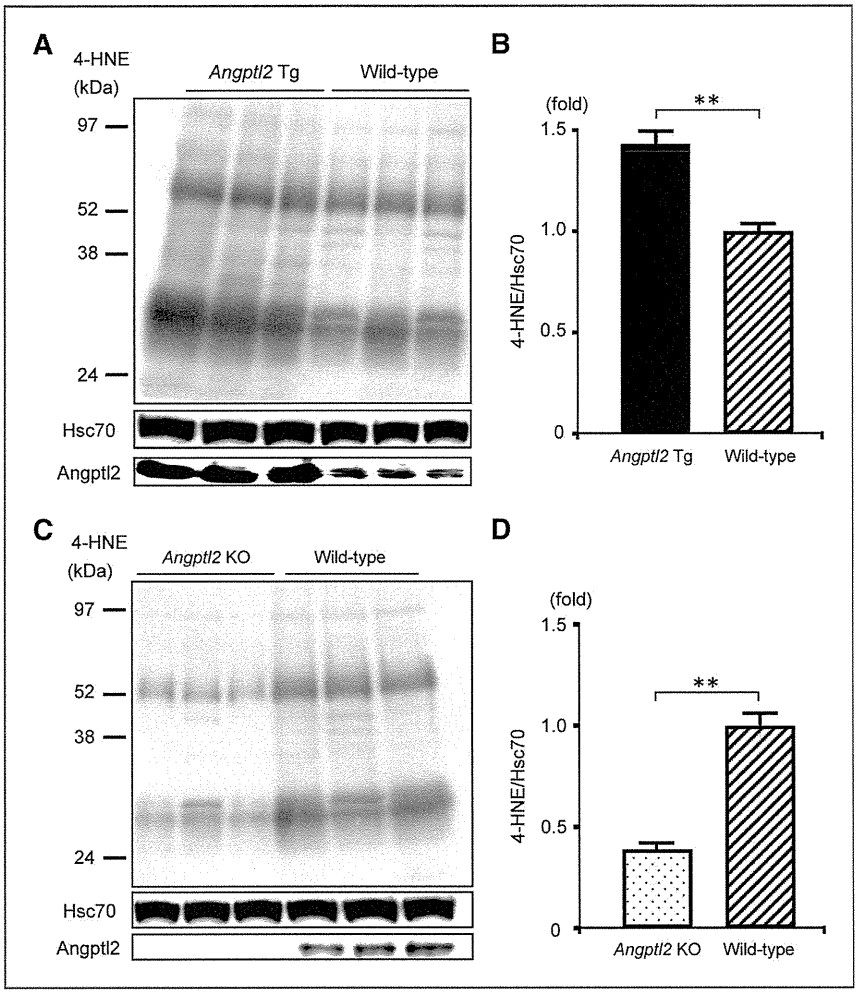

Figure 2. ROS levels increase in skin tissues of K14-*Angptl2* transgenic mice and decrease in tissues from *Angptl2* KO mice. A and C, Western blot analysis using 4-hydroxy-2-nonenal (4-HNE) antibody, which recognizes ROS-modified proteins, of skin tissues of K14-*Angptl2* Tg and wild-type mice (A) and *Angptl2* KO and wild-type mice (C). Skin tissues received a single application of DMBA plus 7 applications of PMA. Hsc70 serves as an internal control. B and D, quantitation of Western blot analysis ($n = 3$) in (B) and (D), (wild-type data set at 1). Graphs show data in the 24 to 97 kDa range. Data are expressed as mean ± SEM. **, $P < 0.01$ compared with wild-type mice.

tissues (data not shown). Therefore, for further study we analyzed skin tissues from the mid-dorsal portion of the back of animals at 7 weeks after beginning chemical application.

In animal tissues, 4-hydroxy-2-nonenal (4-HNE) is a lipid peroxidation product whose formation is closely related to oxidative stress (24). Because of its electrophilic nature, 4-HNE reacts with nucleophilic amino acid residues in proteins to form HNE-adducted proteins. For our studies, we used an HNE-antibody that recognizes HNE-adducted histidine moieties in proteins (HNE-modified proteins) to monitor both the occurrence and extent of oxidative stress in skin tissues (Supplementary Fig. S1). Immunoblot analysis of skin tissues at the 7-week time point using the anti-4-HNE antibody indicated that HNE-modified protein level, in tissues from K14-*Angptl2* Tg mice, significantly increased relative to conditions seen in wild-type mice (Fig. 2A and B). Conversely, levels of HNE-modified proteins in skin tissues of *Angptl2* KO mice were significantly decreased compared with wild-type controls (Fig. 2C and D). In addition, we found that HNE-modified protein levels were positively correlated with the Angptl2 levels (Fig. 2A and C). These findings suggest that Angptl2 increases oxidative stress.

Antioxidant treatment reduces *Angptl2*-associated oxidative stress and decreases papilloma and SCC formation in a SCC model

We previously proposed that Angptl2 expression in skin tissues accelerates chemically induced carcinogenesis by increasing susceptibility to "pre-neoplastic change" and "malignant conversion" (7). To determine whether these changes are attributable to increased oxidative stress in those tissues, we treated mice with the potent antioxidant NAC by including it in their drinking water (25). Immunoblot analysis using anti-4-HNE antibody of skin tissues harvested 7 weeks after initiating chemical application indicated that levels of reactive oxygen species (ROS) in NAC-treated K14-*Angptl2* Tg mice were significantly lower than those seen in Tg mice not treated with NAC (Fig. 3A and B). By 14 weeks

Published OnlineFirst November 20, 2013; DOI: 10.1158/1541-7786.MCR-13-0336

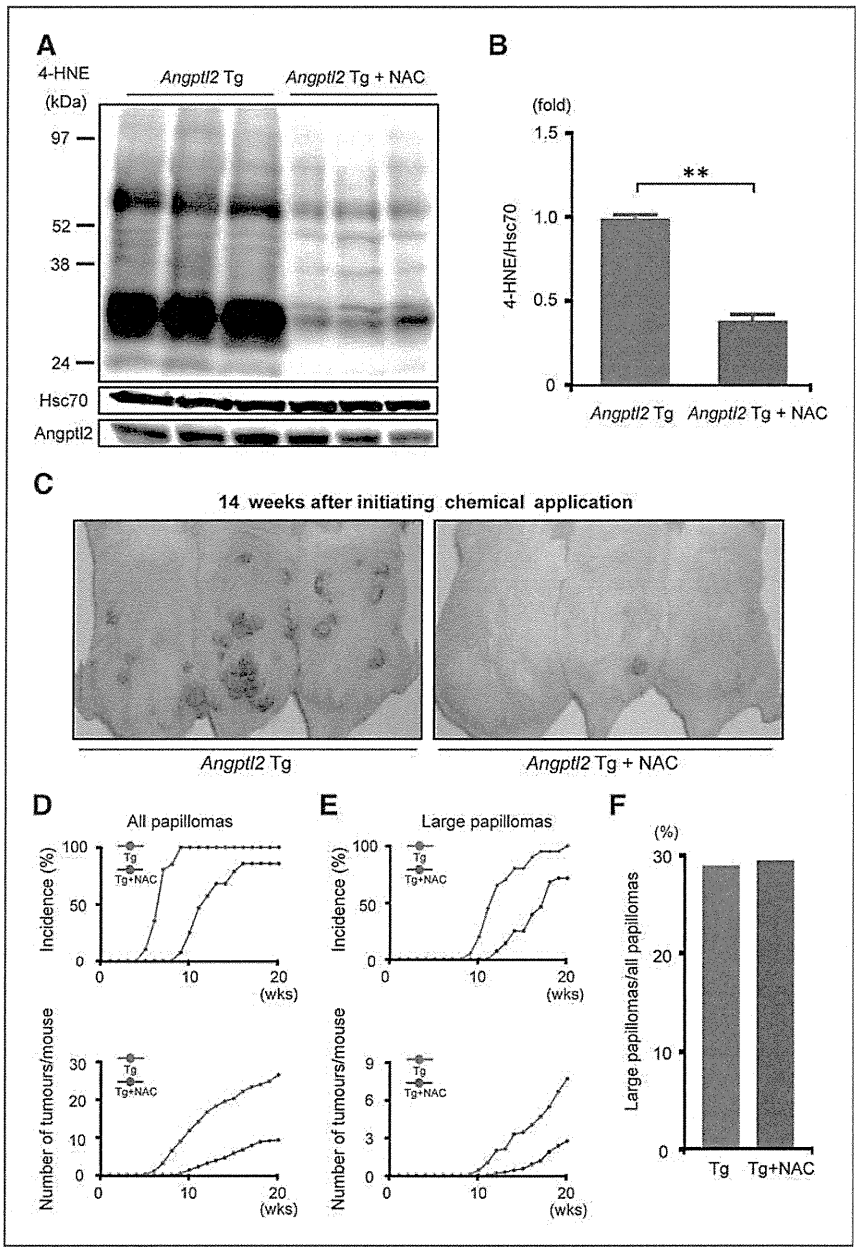

Figure 3. NAC treatment reduces oxidative stress and susceptibility to chemical tumorigenesis in K14-*Angptl2* Tg mice. A and B, Western blot analysis using the 4-hydroxy-2-nonenal (4-HNE) antibody to analyze skin tissues of K14-*Angptl2* Tg mice provided drinking water without (left) or with (right) NAC. Mice were chemically treated as in Fig. 2. Hsc70 serves as an internal control. B, quantitative analysis of Western blot analysis ($n = 3$) of K14-*Angptl2* Tg mice with and without NAC treatment (K14-*Angptl2* Tg without NAC treatment data set at 1). Graphs show data in the 24 to 97 kDa range. Data are expressed as means ± SEM. **, $P < 0.01$ compared with K14-*Angptl2* Tg mice given normal water. C, image showing skin of K14-*Angptl2* Tg mice administered normal (left) and NAC-treated (right) water at 14 weeks after the first chemical application. D and E, top, "incidence" is defined as the percentage of mice with papillomas; bottom, the number of all detectable (1–3 mm) (D) or large (>3 mm) (E) papillomas from K14-*Angptl2* Tg mice provided untreated ($n = 20$; red circles) or NAC-treated ($n = 28$; blue circles) water. $P < 0.005$ from weeks 6 to 20 (in D, bottom), $P < 0.05$ from weeks 10 to 20 (E, bottom). F, proportion of large papillomas seen in K14-*Angptl2* Tg mice provided normal (Tg) or NAC-containing (Tg + NAC) water.

after initiation of chemical treatment, K14-*Angptl2* Tg mice exhibited numerous papillomas in the absence of NAC treatment (Fig. 3C, left), whereas NAC-treated Tg mice showed a significantly reduced number of papillomas (Fig. 3C, right). The average latency is defined as time to reach 50% incidence of all papillomas (7, 26, 27). NAC-treated K14-*Angptl2* mice also showed attenuated formation of skin papillomas, with an average latency of 11 weeks after the beginning of chemical application, as compared with K14-*Angptl2* Tg mice not treated with NAC, which showed an average latency of 7 weeks (Fig. 3D, top). In addition, K14-*Angptl2* Tg mice treated with NAC showed significantly fewer papillomas (Fig. 3D, bottom). After 20 weeks of chemical treatment, NAC-treated K14-*Angptl2* Tg mice exhibited an average of 9.2 papillomas per mouse, whereas K14-*Angptl2* Tg mice without NAC exhibited an average of 26.5 ($P < 1 \times 10^{-9}$). When only large papillomas (diameter > 3 mm) were evaluated, K14-*Angptl2* Tg with treated with

Published OnlineFirst November 20, 2013; DOI: 10.1158/1541-7786.MCR-13-0336

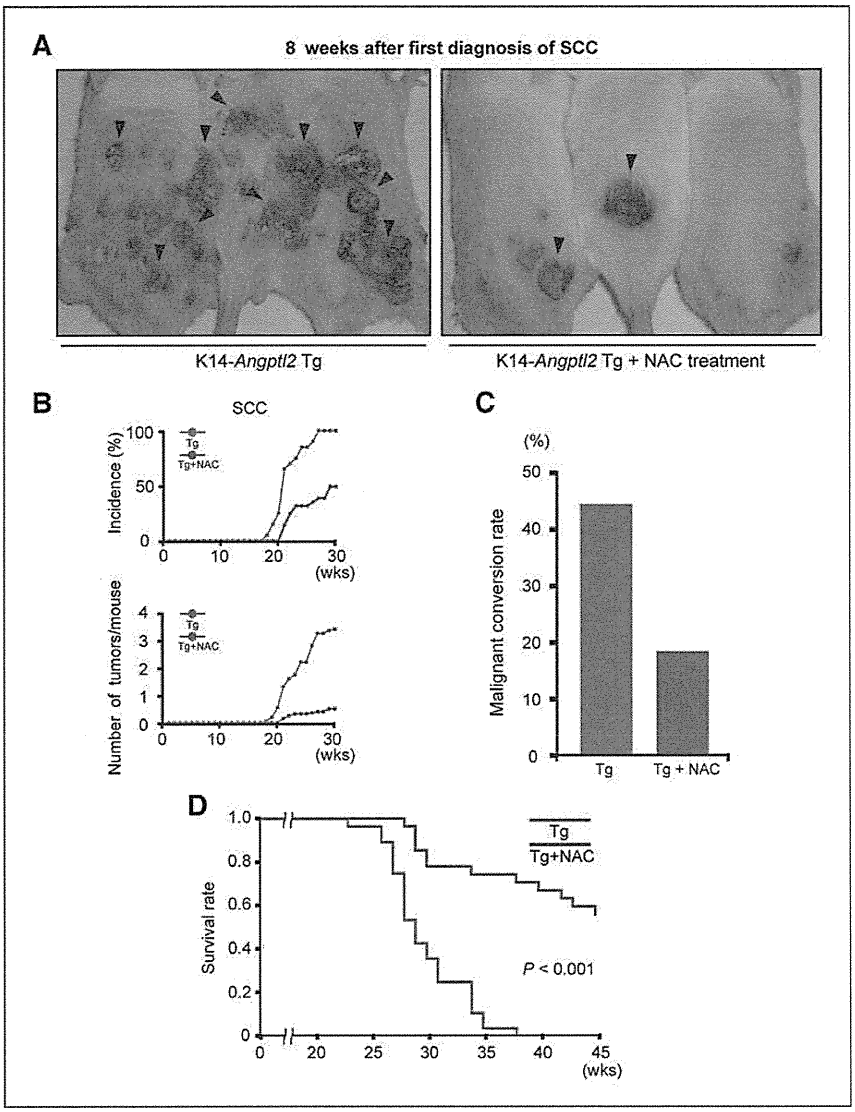

Figure 4. Antioxidant treatment prevents carcinogenesis and prolongs survival of K14-*Angptl2* Tg mice. A, photograph of SCC exhibited by K14-*Angptl2* Tg mice provided normal (left) or NAC-treated (right) water at 8 weeks after first diagnosis of SCC. Arrowheads indicate SCC. B, increased incidence of SCC (top) and number of SCC tumors per mouse (bottom, $P < 0.05$ after week 19) seen in K14-*Angptl2* Tg mice administered normal ($n = 20$; red circles) or NAC-containing ($n = 28$; blue circles) water. C, comparison of the malignant conversion ratio of large papillomas to SCC in K14-*Angptl2* Tg mice provided normal versus NAC-treated water. D, Kaplan–Meier survival curves after initiation of chemical application of K14-*Angptl2* Tg mice provided normal ($n = 28$) or NAC-treated ($n = 27$) water ($P < 0.001$ by log-rank test).

NAC developed papillomas 3 weeks later than did Tg mice without NAC treatment (Fig. 3E, top), and the average number of large papillomas decreased to 0.35-fold that seen in NAC-treated Tg mice (Fig. 3E, bottom). In addition, we performed the same experiments in wild-type mice and confirmed the tumor-inhibitory effect of NAC (Supplementary Fig. S2).

Interestingly, we observed no difference in the ratio of large to total papillomas between mice treated with or without NAC (Fig. 3F), whereas SCC formation was significantly attenuated in NAC-treated versus untreated Tg mice (compare right with left images in Fig. 4A). By 30 weeks after initiation of chemical treatment, 100% of K14-*Angptl2* Tg without NAC treatment had developed malignant SCC, a condition seen in only 50% of NAC-treated mice (Fig. 4B, top). The average number of SCC tumors in NAC-treated K14-*Angptl2* Tg decreased to 0.15-fold relative to untreated Tg mice (Fig. 4B, bottom). The malignant conversion rate, defined as the ratio of the number of SCCs to the number of large papillomas (7, 26, 27), in NAC-treated K14-*Angptl2* Tg mice was lower than that in Tg mice without NAC treatment (Fig. 4C). In addition, survival of NAC-treated Tg mice was significantly prolonged relative to untreated Tg mice (Fig. 4D). Taken together, these results suggest that increased susceptibility to chemically induced skin carcinogenesis seen in this model is attributable to increased ROS production in skin tissues promoted by *Angptl2* overexpression.

Published OnlineFirst November 20, 2013; DOI: 10.1158/1541-7786.MCR-13-0336

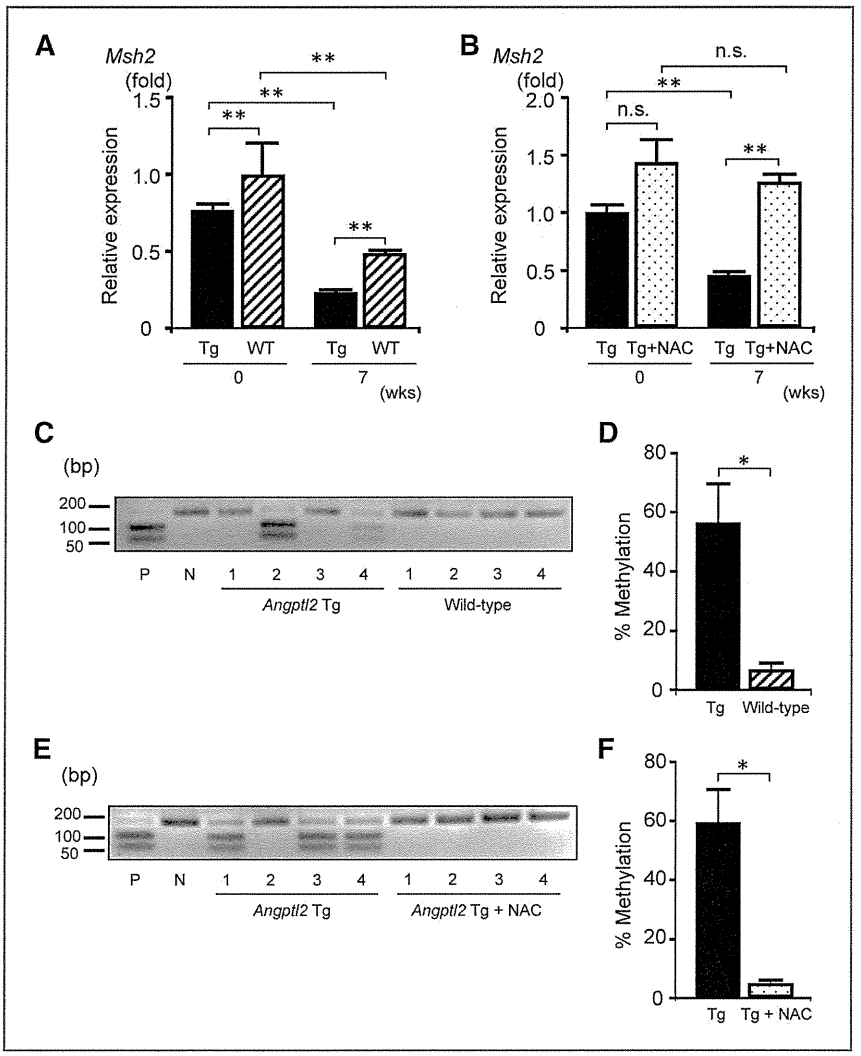

Figure 5. *Angptl2*-dependent hypermethylation of the *Msh2* promoter is ameliorated by antioxidant treatment. A and B, comparative expression levels of *Msh2* in skin tissues ($n = 7$) following a single application of DMBA plus 0 or 7 applications of PMA in K14-*Angptl2* Tg (Tg) versus wild-type (WT) mice (A), and between Tg mice provided normal (Tg) or NAC-treated (Tg + NAC) water (B). Values from wild-type or K14-*Angptl2* Tg without NAC treatment at week 0 data were set at 1. Data are expressed as mean ± SEM. **, $P < 0.01$; n.s., not statistically significant. C and E, representative COBRA methylation analysis following a single application of DMBA plus 7 applications of PMA to skin tissues of K14-*Angptl2* Tg or wild-type mice (C), and to K14-*Angptl2* Tg mice provided normal (*Angptl2* Tg) or NAC-treated (*Angptl2* Tg + NAC) water (E). CpG-methylated NIH 3T3 mouse genomic DNA served as a positive control (P). NIH 3T3 mouse genomic DNA served as a negative control (N). D and F, methylation percentage seen in K14-*Angptl2* Tg ($n = 7$) or wild-type ($n = 7$) mice (D), and in K14-*Angptl2* Tg mice provided normal (*Angptl2* Tg) ($n = 10$) or NAC-treated (*Angptl2* Tg + NAC) water ($n = 10$) (F). Data are expressed as mean ± SEM. **, $P < 0.01$ compared with wild-type mice.

Decreased *Msh2* mRNA levels in skin tissues of K14-*Angptl2* Tg mice are ameliorated by NAC treatment

Because inflammation and oxidative stress downregulate DNA-repair MMR proteins (28, 29), we used quantitative real-time PCR to determine whether Angptl2 alters the expression of *Msh2*, which encodes a MMR protein. *Msh2* expression level assessed prior to oncogenic chemical treatment differed in skin tissues of wild-type and K14-*Angptl2* Tg mice (Fig. 5A). By 7 weeks after initiation of chemical application, *Msh2* expression levels decreased in skin tissues of both K14-*Angptl2* Tg and wild-type mice, although that decrease was significantly greater in tissues from Tg mice (Fig. 5A). In addition, we found that Msh2 expression in skin did not decrease in *Angptl2* KO mice following chemical treatment (Supplementary Fig. S3).

Other DNA repair pathways such as nonhomologous end joining and homologous recombination could underlie rescue of DNA damage in chemical skin carcinogenesis. Therefore, we undertook Western blot analysis to assess levels of DNA-repair enzymes such as Atm and Atr (double- or single-strand breaks), Ku-70, and Ku-80 (nonhomologous end joining), and Rad51 and Brca2 (homologous recombination) in skin of wild-type, K14-*Angptl2*, and *Angptl2* KO mice. We found that, except for Msh2, expression levels of almost all of these factors were similar between wild-type and *Angptl2* KO mice or between *Angptl2* Tg and wild-type mice (Supplementary Figs S4 and S5). These results suggest that the Angptl2-induced decrease in Msh2 protein levels likely plays an important role in carcinogenesis.

Next, we examined whether decreased *Msh2* expression levels seen in K14-*Angptl2* Tg were attributable to increased ROS production in skin tissues. As noted, at 7 weeks after initiation of chemical application, *Msh2* expression levels in skin tissues of K14-*Angptl2* Tg mice had significantly

Published OnlineFirst November 20, 2013; DOI: 10.1158/1541-7786.MCR-13-0336

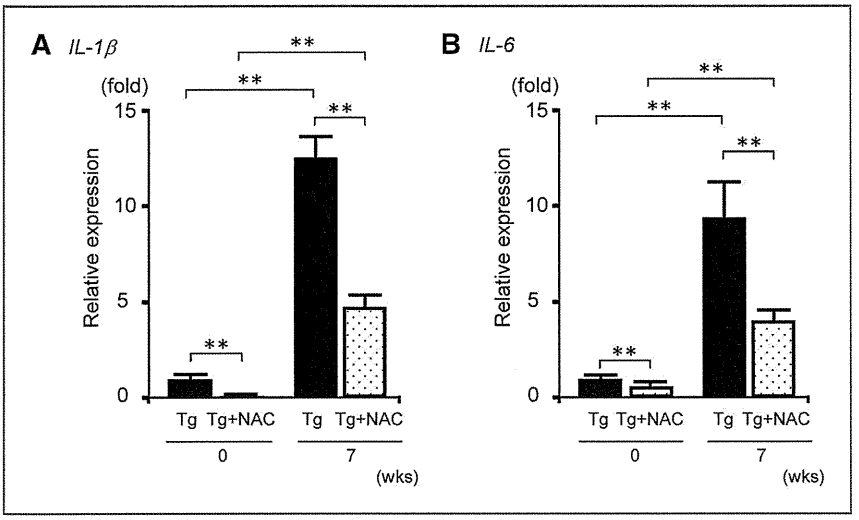

Figure 6. NAC treatment suppresses IL-1β and IL-6 expression in skin tissues following chemical treatment. A and B, comparative expression levels of IL-1β (A) and IL-6 (B) ($n = 7$) after a single application of DMBA plus 0 or 7 applications of PMA to skin tissues of K14-*Angptl2* Tg mice provided normal (Tg) or NAC-treated (Tg + NAC) water. Values from K14-*Angptl2* Tg without NAC treatment at week 0 data were set at 1. Data are expressed as mean ± SEM. **, $P < 0.01$.

decreased, whereas those decreases were ameliorated in Tg mice treated with NAC (Fig. 5B; Supplementary Fig. S6). Protein levels of DNA repair enzymes, except Msh2, were unchanged by NAC treatment (Supplementary Fig. S6). In addition, NAC treatment itself did not increase *Msh2* transcript levels (Supplementary Fig. S7), and decreased *Msh2* expression was ameliorated by NAC treatment of both wild-type and K14-*Angptl2* Tg mice at 7 weeks after initiation of chemical application (Fig. 5B; Supplementary Fig. S7). We conclude that high Angptl2 levels may suppress *Msh2* expression in skin tissues by increasing ROS production.

Methylation of the *Msh2* promoter in skin tissues of K14-*Angptl2* Tg mice decreases following NAC treatment

Oxidative stress has been associated with epigenetic modifications (30–32). Therefore, we asked whether decreased *Msh2* expression seen in skin tissues of K14-*Angptl2* Tg mice was due to oxidative stress and subsequent epigenetic modification of *Msh2*. To do so, we analyzed *Msh2* promoter methylation using COBRA, which provides reliable quantitative results across several DNA methylation levels (17, 33–35). Analysis of restriction digestion patterns of genomic DNA isolated from skin tissues of K14-*Angptl2* Tg mice indicated increased methylation frequency at the *Msh2* promoter, relative to levels seen in wild-type mice (Fig. 5C). Quantitative analysis revealed that approximately 60% of tissue samples from K14-*Angptl2* Tg mice showed high *Msh2* promoter methylation, whereas those levels at the same region of the promoter were seen in only 6.9% of tissue samples from wild-type mice (Fig. 5D). Representative data shown in Fig. 5E indicates that *Msh2* promoter methylation was significantly ameliorated by NAC treatment. Quantitative analysis revealed that NAC treatment decreased *Msh2* promoter methylation in skin tissues of K14-*Angptl2* Tg mice (Fig. 5F) to levels indistinguishable from those seen in wild-type mice (Fig. 5D). We conclude that decreased *Msh2* mRNA expression in skin tissues of K14-*Angptl2* Tg mice is likely attributable to Angptl2-induced oxidative stress and resultant increased *Msh2* promoter methylation.

NAC treatment attenuates Angptl2-induced skin tissue inflammation in a chemically induced SCC model

We previously reported that, based on levels of the proinflammatory factors interleukin (IL)-1β and IL-6, *Angptl2* expression levels in skin tissue are correlated with skin tissue inflammatory status in chemically induced SCC (7). Therefore, we asked whether NAC treatment altered IL-1β and IL-6 expression levels. IL-1β and IL-6 expression was significantly lower in the skin of NAC-treated compared with untreated Tg mice before chemical application (Fig. 6). These findings suggest that NAC treatment decreases inflammation in skin tissues of Tg mice by suppressing ROS production, and that Angptl2-induced inflammation is enhanced by oxidative stress.

MSH2 levels are inversely correlated with ANGPTL2 expression in UV-exposed human skin tissues

Finally, we examined ANGPTL2 and MSH2 expression in UV-exposed human skin tissues. We found that ANGPTL2 expression was low, whereas MSH2 expression was robust in normal skin tissues with minimal sun exposure (Fig. 7A). Although ANGPTL2 expression fluctuated somewhat in cases of actinic keratosis, MSH2 expression was inversely correlated with ANGPTL2 expression (Fig. 7B; Supplementary Fig. S8). In addition, ANGPTL2 expression was robust and MSH2 expression was weak in tissue of sun-exposed squamous cell carcinoma (Fig. 7C). These results suggest that UV exposure induces ANGPTL2 expression, leading to decreases MSH2 levels in human skin tissues.

Discussion

Our previous findings that K14-*Angptl2* Tg mice do not show papillomas or carcinomas when mice are treated with a tumor promoter (PMA) alone (7) indicate that Angptl2 is not an oncogene. However, we concluded that increased

Published OnlineFirst November 20, 2013; DOI: 10.1158/1541-7786.MCR-13-0336

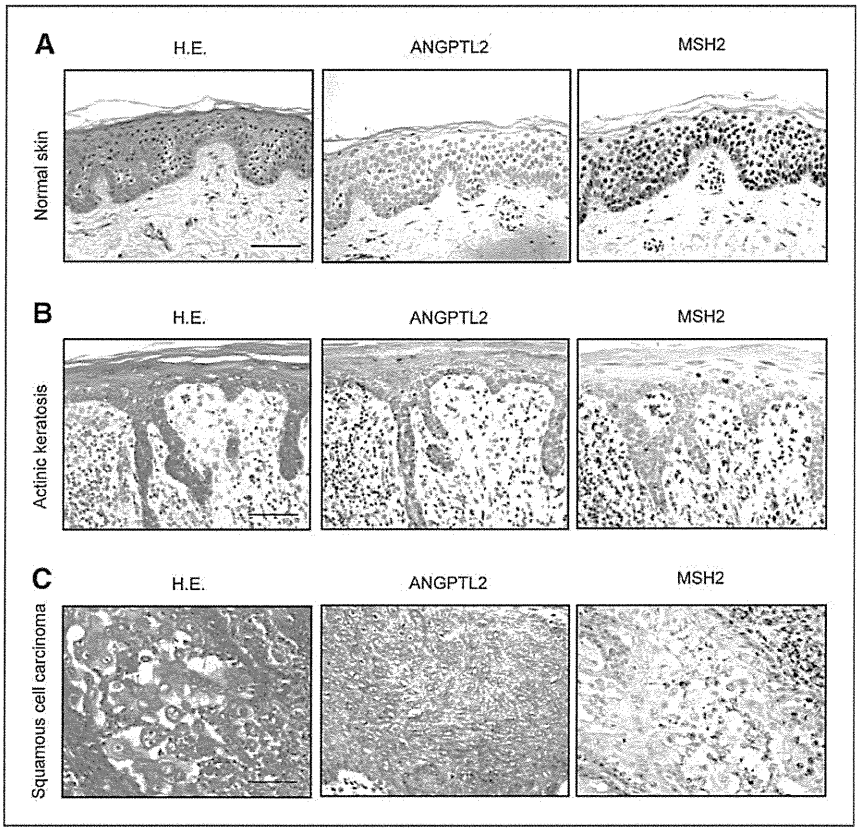

Figure 7. ANGPTL2 and MSH2 expression levels in normal skin, actinic keratosis, and squamous cell carcinoma. A–C, representative photographs of hematoxylin and eosin staining and immunohistochemical analysis with ANGPTL2 and MSH2 antibodies in normal human abdominal skin (non–sun-exposed area) (A), actinic keratosis on the face (sun-exposed area) (B), and SCC on the face (sun-exposed area) (C). Scale bars, 500 μm.

Angptl2 expression in skin tissue increases inflammation and accelerates carcinogenesis by enhancing susceptibility to both "pre-neoplastic change" and "malignant conversion." Our conclusion was based on studies using a skin carcinogenesis mice model employing DMBA/PMA treatment (7), a well-characterized model in which an initiating oncogenic mutation is followed by accumulation of additional oncogenic mutations (8–10). Findings reported here suggest that Angptl2 expression induces skin inflammation and likely accelerates acquisition of oncogenic mutations resulting in carcinogenesis. In addition, we find that in skin tissues Angptl2 overexpression correlates with decreased *Msh2* expression, likely due to methylation of its promoter region triggered by ROS accumulation in those tissues. Conversely, we show that continuous treatment with the antioxidant NAC reduces ROS accumulation in skin tissues and ameliorates decreased *Msh2* expression due to epigenetic modification, decreasing susceptibility to carcinogenesis. Finally, we report that antioxidant treatment also decreases skin tissue inflammation in K14-*Angptl2* Tg mice by suppressing ROS production, suggesting that Angptl2-induced inflammation is enhanced under oxidative stress conditions. Overall, we conclude that enhanced oxidative stress and chronic inflammation induced by Angptl2 synergize to increase susceptibility for carcinogenesis.

Currently, we do not know the mechanism underlying enhanced ROS production in skin tissue expressing excess Angptl2. Our previous report showing chronic inflammation in skin tissue of K14-*Angptl2* Tg mice demonstrated infiltration of skin tissue by inflammatory cells, including activated macrophages and neutrophils (7), both of which are sources of ROS (36). Angptl2 reportedly activates NF-κB proinflammatory signaling in various cell types (3–7, 37), which also enhances ROS production (38). Taken together, Angptl2 secreted from skin tissue of K14-*Angptl2* Tg mice may increase ROS production due to activity of infiltrated and activated inflammatory cells.

In addition, we demonstrate here decreased *Msh2* expression in skin tissues of K14-*Angptl2* Tg mice, most likely due to methylation of the *Msh2* promoter, an activity significantly improved by NAC treatment. Thus increased oxidative stress caused by *Angptl2* overexpression may promote *Msh2* promoter methylation. Previously, others have reported that ROS promotes development of human carcinogenesis through epigenetic regulation of gene expression (32). For example, ROS-induced oxidative stress reportedly silences promoters of tumor suppressors via hypermethylation (39). In addition, ROS induces Snail, which activates histone deacetylase 1 and DNA methyltransferase 1 (40). Moreover, we have

Published OnlineFirst November 20, 2013; DOI: 10.1158/1541-7786.MCR-13-0336

reported induction of an epithelial-to-mesenchymal transition (EMT) by increasing *Snail* mRNA expression and activating the TGF-β pathway in SCC of K14-*Angptl2* Tg mice (7), suggesting that Snail functions in *Msh2* promoter methylation. Further, ROS promotes phosphorylation of the transcription factors c-Jun and ATF2, increasing expression of their target genes (41). Interestingly, we reported that c-Jun and ATF2 activity increases Angptl2 expression (6), suggesting a mechanism through which ROS might increase Angptl2 expression.

We conclude that Angptl2 accelerates susceptibility to both "preneoplastic change" and "malignant conversion" by activating a cycle of chronic Inflammation and oxidative stress in the premalignant tissue microenvironment (Supplementary Fig. S9). More recently, we observed that spontaneous carcinogenesis is significantly decreased in *Angptl2* KO compared with wild-type mice (our unpublished data), suggesting that Angptl2 contributes not only to chemically induced carcinogenesis but also to various types of spontaneous cancers. Overall, our findings suggest that Angptl2 represents a target to develop new strategies to antagonize these activities in premalignant tissue.

Disclosure of Potential Conflicts of Interest

No potential conflicts of interest were disclosed.

Authors' Contributions

Conception and design: J. Aoi, M. Endo, H. Ihn, Y. Oike
Development of methodology: M. Endo, K. Miyata, H. Horiguchi, S. Hirakawa, H. Ihn
Acquisition of data (provided animals, acquired and managed patients, provided facilities, etc.): J. Aoi, M. Endo, A. Ogata
Analysis and interpretation of data (e.g., statistical analysis, biostatistics, computational analysis): J. Aoi, M. Endo, T. Kadomatsu, T. Masuda, S. Hirakawa, H. Ihn,
Writing, review, and/or revision of the manuscript: J. Aoi, M. Endo, S. Fukushima, S. Hirakawa, T. Sawa, H. Ihn, Y. Oike
Administrative, technical, or material support (i.e., reporting or organizing data, constructing databases): M. Endo, H. Odagiri, S. Fukushima, M. Jinnin, T. Akaike
Study supervision: M. Endo, K. Miyata, S. Fukushima, S. Hirakawa, H. Ihn, Y. Oike

Acknowledgments

The authors thank S. Iwaki, Y. Indoh, R. Shindo, and M. Nakata for providing technical assistance.

Grant Support

This work was financially supported by Grants-in-Aid for Scientific Research on Priority Areas from the Ministry of Education, Culture, Sports, Science and Technology of Japan, by the Japan Society for the Promotion of Science (JSPS) through its Funding Program for Next Generation World-Leading Researchers (NEXT Program), and a research program of the Project for Development of Innovative Research on Cancer Therapeutics (P-Direct), Ministry of Education, Culture, Sports, Science and Technology of Japan, and the Core Research for Evolutional Science and Technology (CREST) program of Japan Science and Technology Agency (JST), and by grants from the Takeda Science Foundation and the Yasuda Medical Foundation.

The costs of publication of this article were defrayed in part by the payment of page charges. This article must therefore be hereby marked *advertisement* in accordance with 18 U.S.C. Section 1734 solely to indicate this fact.

Received June 27, 2013; revised October 7, 2013; accepted October 28, 2013; published OnlineFirst November 20, 2013.

References

1. Balkwill F, Mantovani A. Inflammation and cancer: back to Virchow? Lancet 2001;357:539–45.
2. Mantovani A, Allavena P, Sica A, Balkwill F. Cancer-related inflammation. Nature 2008;454:436–44.
3. Tabata M, Kadomatsu T, Fukuhara S, Miyata K, Ito Y, Endo M, et al. Angiopoietin-like protein 2 promotes chronic adipose tissue inflammation and obesity-related systemic insulin resistance. Cell Metab 2009;10:178–88.
4. Okada T, Tsukano H, Endo M, Tabata M, Miyata K, Kadomatsu T, et al. Synoviocyte-derived angiopoietin-like protein 2 contributes to synovial chronic inflammation in rheumatoid arthritis. Am J Pathol 2010; 176:2309–19.
5. Ogata A, Endo M, Aoi J, Takahashi O, Kadomatsu T, Miyata K, et al. The role of angiopoietin-like protein 2 in pathogenesis of dermatomyositis. Biochem Biophys Res Commun 2012;418:494–9.
6. Endo M, Nakano M, Kadomatsu T, Fukuhara S, Kuroda H, Mikami S, et al. Tumor cell-derived angiopoietin-like protein ANGPTL2 is a critical driver of metastasis. Cancer Res 2012;72:1784–94.
7. Aoi J, Endo M, Kadomatsu T, Miyata K, Nakano M, Horiguchi H, et al. Angiopoietin-like protein 2 is an important facilitator of inflammatory carcinogenesis and metastasis. Cancer Res 2011;71: 7502–12.
8. Knudson AG. Two genetic hits (more or less) to cancer. Nat Rev Cancer 2001;1:157–62.
9. Hanahan D, Weinberg RA. Hallmarks of cancer: the next generation. Cell 2011;144:646–74.
10. Fearon ER, Vogelstein B. A genetic model for colorectal tumorigenesis. Cell 1990;61:759–67.
11. Glickman BW, Radman M. Escherichia coli mutator mutants deficient in methylation-instructed DNA mismatch correction. Proc Natl Acad Sci U S A 1980;77:1063–7.
12. Radman M, Wagner R. Mismatch repair in Escherichia coli. Annu Rev Genet 1986;20:523–38.
13. Modrich P. Methyl-directed DNA mismatch correction. J Biol Chem 1989;264:6597–600.
14. Modrich P, Lahue R. Mismatch repair in replication fidelity, genetic recombination, and cancer biology. Annu Rev Biochem 1996;65: 101–33.
15. Jun SH, Kim TG, Ban C. DNA mismatch repair system. Classical and fresh roles. FEBS J 2006;273:1609–19.
16. Umar A, Boland CR, Terdiman JP, Syngal S, de la Chapelle A, Rüschoff J, et al. Revised Bethesda Guidelines for hereditary nonpolyposis colorectal cancer (Lynch syndrome) and microsatellite instability. J Natl Cancer Inst 2004;96:261–8.
17. Conde-Perezprina JC, Luna-Lopez A, Lopez-Diazguerrero NE, Damian-Matsumura P, Zentella A, Konigsberg M. Msh2 promoter region hypermethylation as a marker of aging-related deterioration in old retired female breeder mice. Biogerontology 2008;9:325–34.
18. Harfe BD, Jinks-Robertson S. Sequence composition and context effects on the generation and repair of frameshift intermediates in mononucleotide runs in Saccharomyces cerevisiae. Genetics 2000; 156:571–8.
19. Campbell MR, Wang Y, Andrew SE, Liu Y. Msh2 deficiency leads to chromosomal abnormalities, centrosome amplification, and telomere capping defect. Oncogene 2006;25:2531–6.
20. Hawighorst T, Oura H, Streit M, Janes L, Nguyen L, Brown LF, et al. Thrombospondin-1 selectively inhibits early-stage carcinogenesis and angiogenesis but not tumor lymphangiogenesis and lymphatic metastasis in transgenic mice. Oncogene 2002;21:7945–56.
21. Hawighorst T, Velasco P, Streit M, Hong YK, Kyriakides TR, Brown LF, et al. Thrombospondin-2 plays a protective role in multistep carcinogenesis: a novel host anti-tumor defense mechanism. EMBO J 2001; 20:2631–40.
22. Kirkham N. Tumors and Cysts of the Epidermis. In: David E., Elder, et al. editors. Lever's Histopathology of the Skin. Philadelphia: Lippincott Williams & Wilkins; 2009. p. 791–849.

Published OnlineFirst November 20, 2013; DOI: 10.1158/1541-7786.MCR-13-0336

23. Garcia-Manero G, Daniel J, Smith TL, Kornblau SM, Lee MS, Kantarjian HM, et al. DNA methylation of multiple promoter-associated CpG islands in adult acute lymphocytic leukemia. Clin Cancer Res 2002; 8:2217–24.
24. Uchida K. 4-Hydroxy-2-nonenal: a product and mediator of oxidative stress. Prog Lipid Res 2003;42:318–43.
25. Yano M, Watanabe K, Yamamoto T, Ikeda K, Senokuchi T, Lu M, et al. Mitochondrial dysfunction and increased reactive oxygen species impair insulin secretion in sphingomyelin synthase 1-null mice. J Biol Chem 2011;286:3992–4002.
26. Hirakawa S, Brown LF, Kodama S, Paavonen K, Alitalo K, Detmar M. VEGF-C-induced lymphangiogenesis in sentinel lymph nodes promotes tumor metastasis to distant sites. Blood 2007;109:1010–7.
27. Hirakawa S, Kodama S, Kunstfeld R, Kajiya K, Brown LF, Detmar M. VEGF-A induces tumor and sentinel lymph node lymphangiogenesis and promotes lymphatic metastasis. J Exp Med 2005;201:1089–99.
28. Colotta F, Allavena P, Sica A, Garlanda C, Mantovani A. Cancer-related inflammation, the seventh hallmark of cancer: links to genetic instability. Carcinogenesis 2009;30:1073–81.
29. Hsu T, Huang KM, Tsai HT, Sung ST, Ho TN. Cadmium(Cd)-induced oxidative stress down-regulates the gene expression of DNA mismatch recognition proteins MutS homolog 2 (MSH2) and MSH6 in zebrafish (Danio rerio) embryos. Aquat Toxicol 2013;126:9–16.
30. Grivennikov SI, Greten FR, Karin M. Immunity, inflammation, and cancer. Cell 2010;140:883–99.
31. Valko M, Rhodes CJ, Moncol J, Izakovic M, Mazur M. Free radicals, metals and antioxidants in oxidative stress-induced cancer. Chem Biol Interact 2006;160:1–40.
32. Campos AC, Molognoni F, Melo FH, Galdieri LC, Carneiro CR, D'Almeida V, et al. Oxidative stress modulates DNA methylation during melanocyte anchorage blockade associated with malignant transformation. Neoplasia 2007;9:1111–21.
33. Xiong Z, Laird PW. COBRA: a sensitive and quantitative DNA methylation assay. Nucleic Acids Res 1997;25:2532–4.
34. Grunau C, Sanchez C, Ehrlich M, van der Bruggen P, Hindermann W, Rodriguez C, et al. Frequent DNA hypomethylation of human juxtacentromeric BAGE loci in cancer. Genes Chromosomes Cancer 2005;43:11–24.
35. Goldberg M, Rummelt C, Laerm A, Helmbold P, Holbach LM, Ballhausen WG. Epigenetic silencing contributes to frequent loss of the fragile histidine triad tumour suppressor in basal cell carcinomas. Br J Dermatol 2006;155:1154–8.
36. Klaunig JE, Kamendulis LM. The role of oxidative stress in carcinogenesis. Annu Rev Pharmacol Toxicol 2004;44:239–67.
37. Tazume H, Miyata K, Tian Z, Endo M, Horiguchi H, Takahashi O, et al. Macrophage-derived angiopoietin-like protein 2 accelerates development of abdominal aortic aneurysm. Arterioscler Thromb Vasc Biol 2012;32:1400–9.
38. Kundu JK, Surh YJ. Inflammation: gearing the journey to cancer. Mutat Res 2008;659:15–30.
39. Ziech D, Franco R, Pappa A, Panayiotidis MI. Reactive oxygen species (ROS)–induced genetic and epigenetic alterations in human carcinogenesis. Mutat Res 2011;711:167–73.
40. Lim SO, Gu JM, Kim MS, Kim HS, Park YN, Park CK, et al. Epigenetic changes induced by reactive oxygen species in hepatocellular carcinoma: methylation of the E-cadherin promoter. Gastroenterology 2008;135:2128–40, 40 e1–8.
41. Klaunig JE, Wang Z, Pu X, Zhou S. Oxidative stress and oxidative damage in chemical carcinogenesis. Toxicol Appl Pharmacol 2011; 254:86–99.

DOI: 10.1111/exd.12238
www.wileyonlinelibrary.com/journal/EXD

Letter to the Editor

Serum levels of leptin receptor in patients with malignant melanoma as a new tumor marker

Hironori Mizutani, Satoshi Fukushima, Shinichi Masuguchi, Junji Yamashita, Azusa Miyashita, Satoshi Nakahara, Jun Aoi, Yuji Inoue, Masatoshi Jinnin and Hironobu Ihn

Department of Dermatology and Plastic Surgery, Faculty of Life Sciences, Kumamoto University, Kumamoto, Japan
Correspondence: Satoshi Fukushima, MD, PhD, Department of Dermatology and Plastic Surgery, Faculty of Life Sciences, Kumamoto University, Honjo 1-1-1, Kumamoto 860-8556, Japan, Tel.: +81 96 373 5233, Fax +81 96 373 5235, e-mail: satoshi.fukushima.tb@gmail.com

Abstract: Leptin is known to be abnormally expressed in a variety of cancers, and leptin receptors have been reported to be expressed on human melanoma cells. In this study, we evaluated the possibility that the serum levels of leptin receptor could be a tumor marker of malignant melanoma (MM). Serum samples were obtained from 71 patients with MM, and the serum levels of leptin receptor were measured by double-determinant ELISA. Interestingly, serum levels of leptin receptor decreased gradually with the stages of MM, being highest at *in situ* and lowest at stage IV. There was also a trend of reverse correlation between tumor thickness and serum levels of leptin receptor. To our knowledge, this is the first report investigating the serum levels of leptin receptor in MM, and serum leptin receptor levels may be used as a useful tumor marker of MM.

Key words: leptin – leptin receptor – malignant melanoma – tumor marker

Accepted for publication 9 September 2013

Background

Malignant melanoma (MM) is an aggressive neoplasm that can be fatal, especially if it metastasizes. Therefore, it is very important to reduce the fatality rate by early diagnosis and better diagnostic tools. However, there are few tumor markers for MM.

Leptin has been identified as a central mediator that regulates energy intake and expenditure, including appetite, metabolism and fat storage (1). Epidemiological studies have indicated that obesity is associated with a higher risk for certain cancers caused by elevated levels of adipocyte-derived hormones. It has been reported that leptin is overexpressed in ovarian cancer (2) and breast cancer (3,4). On the other hand, leptin inhibits hepatocellular carcinoma proliferation (1,5).

Several papers have reported the relationship between leptin and MM. The risk for developing MM was found to be positively associated with serum levels of leptin and inversely with healthy lifestyle factors (6). Melanoma tumor growth may be accelerated by leptin (7).

Questions addressed

In this study, we first investigated the serum levels of leptin receptor in patients with MM and evaluated the possibility that serum levels of leptin receptor could be a useful marker for MM.

Experimental design

Serum samples were obtained from 71 patients with MM (33 men, 38 women). Control serum samples were also collected from 16 healthy volunteers. Human leptin receptors in the sera of patients with MM were measured using a commercial kit (Human Leptin Receptor ELISA; BioVendor R & D, Brno, Czech Republic). The detailed methodologies are described in the Data S1.

Results

Serum levels of leptin receptor in patients with MM were classified based on the American Joint Committee on Cancer (AJCC) staging (Fig. 1a). There were significant differences in the values between healthy controls and the patients with stage III MM or those with stage IV. Serum levels of leptin receptor decreased gradually with the stages of MM, being highest at *in situ* and lowest at stage IV. There was a significant difference in the values between healthy controls and the patients with invasive MM of all subtypes (Fig. 1b). When the patients were classified into melanoma subtypes, serum levels of leptin receptor in patients with nodular melanoma and mucosal MM were significantly lower than those with acral lentiginous melanoma or those with lentigo maligna melanoma. When the patients with MM were divided into two groups according to the tumor thickness (<2 mm or >2 mm), there was significant difference in the serum levels of leptin receptor between the two groups ($P = 0.0016$) (Figure S1).

The rates of decreased serum leptin receptor concentrations under the cut-off value were higher than those of increased serum 5-S-CD concentrations in patients with stage *in situ*, III and IV MM patients and in all MM patients (Table 1). When the cut-off value was set at the mean – 2SD of the healthy controls, decreased serum levels of leptin receptor were found in 28 of the 71 MM patients (39.4%). The sensitivities of decreased serum leptin receptor levels in stage *in situ*, III and IV patients were 25.0%, 75.0% and 100%, respectively. The area under the curves was 0.714 (95% CI, 0.59 to 0.84) (Figure S2). Serum samples were obtained from six MM patients who had experienced excisions of primary melanoma but who had developed a recurrence during the follow-up period. We found in 5 of the 6 patients that the serum levels were decreased at the point of recurrence (Figure S3). These results suggested that the serum levels of leptin receptor might serve as a useful biomarker for the detection of melanoma.

Conclusions

Serum levels of leptin are closely correlated with adiposity in humans (8,9). In this study, serum levels of leptin receptor did not show any correlation with BMI in patients with melanoma (data not shown). In the setting of obesity, the body becomes resistant to the effects of leptin, resulting in paradoxical weight gain in the setting of high levels of circulating leptin (10). It has been shown that there is strong negative correlation between serum levels of leptin and leptin

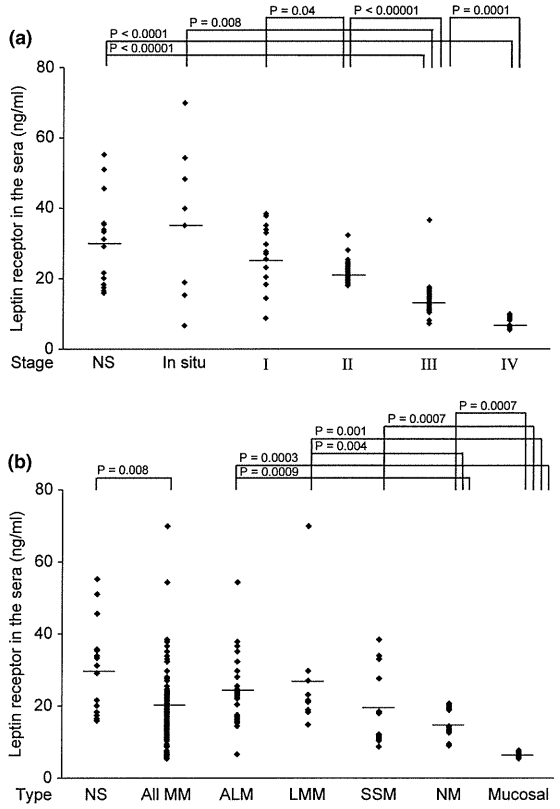

Figure 1. (a) Serum levels of leptin receptor in patinents with malignant melanoma (MM) *in situ*, patients with MM stages I – IV and normal subjects (NS). Bars show means. Staging was based on AJCC classification. Serum leptin receptor levels were measured with ELISA. (b). The serum levels of leptin receptor measured by ELISA in patients with different malignant melanoma (MM) subtypes {28 had acral lentiginous MM (ALM), 11 had lentigo maligna MM (LMM), 12 had superficial spreading MM (SSM), 12 had nodular MM (NM) or 6 had mucosal MM} and in normal subjects (NS). Bars show means. Serum leptin receptor levels were measured with ELISA. The Mann-Whitney test was used for analysis.

receptor in patients with non-alcoholic fatty liver disease (11). These findings point out to insulin resistance as a potentially independent risk factor for melanoma (12). Leptin receptor was expressed on human melanoma cells (13). In this study, we expected that there was a significant increase in serum leptin receptor levels in patients with MM. Surprisingly, the serum levels of leptin receptor decreased

Table 1. The rates of decreased serum leptin receptor concentrations under the cut-off value (the mean – 2SD of healthy controls) and those of serum 5-S-CD concentrations over 10 nM

Stage	Decreased leptin receptor (%)	Increased 5-S-CD (%)
In situ	2/8 (25.0)	0/8 (0.0)
I	2/15 (13.3)	3/15 (20.0)
II	0/19 (0.0)	0/19 (0.0)
III	15/20 (75.0)	1/20 (5.0)
IV	9/9 (100)	6/9 (66.7)
Total	28/71 (39.4)	10/71 (14.1)

gradually from stage I to stage IV. The mechanism is not clear yet, but we speculate that there may be negative feedback mechanism regulating the expression of leptin receptor. The expression of leptin receptor might decrease in normal cells, even though melanoma cells express leptin receptor. Similar results were also observed in breast cancer (6). On the other hand, there have been previous reports showing the opposite results (14, 15). Additionally, the expression levels of leptin receptor in the culture medium of human melanoma cell lines were relatively low (Figure S4). These results are consistent with our findings that the serum levels of leptin receptor decreased gradually with the stages of MM, being highest at *in situ* and lowest at stage IV. Furthermore, we examined serum levels of leptin receptor in 16 patients with cutaneous angiosarcoma. There was no significant difference in serum levels of leptin receptor in the patients with cutaneous angiosarcoma with or without metastasis (data not shown). Serum levels of leptin receptor with disease progression might vary in the types of cancers.

In conclusion, we showed the possibility that leptin receptor is associated with the progression of MM. Our results may provide clues to clarify the pathogenesis of MM.

Acknowledgements

This work was supported by JSPS Grant-in-Aid for Young Scientists (B) 23791280 and the National Cancer Center Research and Development Fund (23-A-22).

Author contributions

H. Mizutani performed the experiments, analysed the data and wrote the manuscript. S. Fukushima designed the research study and wrote the manuscript. S. Masuguchi, J. Yamashita, A. Miyashita and S. Nakahara contributed to the experiments using cultured cells and the data analysis. J. Aoi, Y. Inoue and M Jinnin gave excellent scientific suggestion and contributed to writing the manuscript. H. Ihn contributed to the design of the experiments.

Conflict of interest

The authors have declared no conflicting interests.

References

1 Thompson K J, Lau K N, Johnson S *et al.* HPB (Oxford) 2011: **13**: 225–233.
2 Ptak A, Kolaczkowska E, Gregoraszczuk E L. Endocrine 2013: **43**: 394–403.
3 Barone I, Catalano S, Gelsomino L *et al.* Cancer Res 2012: **72**: 1416–1427.
4 Jeong Y J, Bong J G, Park S H *et al.* J Breast Cancer 2011: **14**: 96–103.
5 Wang S N, Lee K T, Ker C G. World J Gastroenterol 2010: **16**: 5801–5809.
6 Gogas H, Trakatelli M, Dessypris N *et al.* Ann Oncol 2008: **19**: 384–389.
7 Brandon E L, Gu J W, Cantwell L *et al.* Cancer Biol Ther 2009: **8**: 1871–1879.
8 Xue K, Liu H, Jian Q *et al.* Exp Dermatol 2013: **22**: 406–410.
9 Gerdes S, Osadtschy S, Rostami-Yazdi M *et al.* Exp Dermatol 2012: **21**: 43–47.
10 Zhang Y, Scarpace P J. Physiol Behav 2006: **88**: 249–256.
11 Huang X D, Fan Y, Zhang H *et al.* World J Gastroenterol 2008: **14**: 2888–2893.
12 Antoniadis A G, Petridou E T, Antonopoulos C N *et al.* Melanoma Res 2011: **21**: 541–546.
13 Ellerhorst J A, Diwan A H, Dang S M *et al.* Oncol Rep 2010: **23**: 901–907.
14 Ishikawa M, Kitayama J, Nagawa H *et al.* Clin Cancer Res 2004: **10**: 4325–4531.
15 Horiguchi A, Sumitomo M, Asakuma J *et al.* J Urol 2006: **176**: 1631–1635.

Supporting Information

Additional Supporting Information may be found in the online version of this article:

Figure S1. Serum levels of leptin receptor in patients with MM with tumor thickness <2 mm and those with thickness >2 mm as measured with ELISA.

Figure S2. ROC curves for expressions of leptin receptor to distinguish the patients with MM from the healthy controls.

Figure S3. The longitudinal study of serum leptin receptor levels in six MM patients who had experienced excisions of primary melanoma but who had developed a recurrence during the follow-up period.

Figure S4. Four kinds of human melanoma cells (MM-LH, 164mel, SK-MEL28, MeWo) were cultured (10^5 cells/well in 200 μl, 48 h) in 96-well culture plates and the culture medium was measured by double-determinant ELISA.

Data S1. Supplemental methods.

別紙４

研究成果の刊行に関する一覧表

研究代表者　京都大学ウイルス研究所　教授　松岡雅雄
研究分担者　川崎医科大学　微生物学　教授　齊藤峰輝

書籍

著者氏名	論文タイトル名	書籍全体の編集者名	書　籍　名	出版社名	出版地	出版年	ページ
Saito M	HTLV-1.	Stanley Maloy, Kelly Hughes	**Encyclopedia of Genetics 2nd Edition**	Elsevier	Oxford, UK	2013	543-545

雑誌

発表者氏名	論文タイトル名	発表誌名	巻号	ページ	出版年
Saito M, Tanaka R, Arishima S, Matsuzaki T, Ishihara S, Tokashiki T, Ohya Y, Takashima H, Umehara F, Izumo S, Tanaka Y.	Increased expression of OX40 is associated with progressive disease in patients with HTLV-1-associated myelopathy/tropical spastic paraparesis.	**Retrovirology.**	10	51	2013
Kodama A, Tanaka R, **Saito M,** Ansari AA, Tanaka Y.	A novel and simple method for generation of human dendritic cells from unfractionated peripheral blood mononuclear cells within 2 days: its application for induction of HIV-1-reactive CD4 (+) T cells in the hu-PBL SCID mice.	**Front Microbiol.**	4	292	2013
Saito M	Neuroimmunological aspects of human T cell leukemia virus type 1-associated myelopathy/tropical spastic paraparesis.	**J Neurovirol.**	20	164-174	2014
Tanaka Y, Takahashi Y, Tanaka R, Kodama A, Fujii H, Hasegawa A, Kannagi M, Ansari AA, **Saito M.**	Elimination of human T cell leukemia virus type-1-infected cells by neutralizing and antibody-dependent cellular cytotoxicity-inducing antibodies against human T cell leukemia virus type-1 envelope gp46.	**AIDS Res Hum Retroviruses.**		in press	2014
Saito M	Pathogenic conversion of Foxp3+ T cells into Th17 cells: is this also the case for multiple sclerosis?	**Clin Exp Neuroimmunol.**		in press	2014

HTLV-1

M Saito, University of the Ryukyus, Okinawa, Japan

This article is a revision of the previous edition article by MJS Dyer, volume 1, p 979, © 2001, Elsevier Inc.

Glossary

Cytotoxic T cell A cytotoxic T cell belongs to a subgroup of T lymphocytes with CD8 receptor that are antigen- specific and capable of inducing the death of virus-infected somatic or tumor cells.

Gliosis Gliosis is the process of scarring in the central nervous system, caused by a proliferation of astrocytes.

Oligoclonal band Oligoclonal bands are bands of immunoglobulins that are seen when a blood serum (or plasma) or cerebrospinal fluid (CSF) is analyzed by protein electrophoresis. The presence of oligoclonal bands in CSF but not in blood serum (or plasma) means the production of immunoglobulins in central nervous system, that is, inflammation in the central nervous system.

Provirus A provirus is the form of the virus which is capable of being integrated into the chromosome of the host cell.

Spastic paraparesis Mild or moderate loss of motor function accompanied by spasticity in the extremities mainly caused by central nervous system (brain and spinal cord) diseases.

Human T-lymphotropic virus type-1 (HTLV-1) belongs to the *Deltaretrovirus* genus of the Orthoretrovirinae subfamily and infects 10–20 million people worldwide. HTLV-1 can be transmitted through sexual contact, intravenous drug use, and breastfeeding from mother to child. The infection is endemic in southwest Japan, the Caribbean, sub-Saharan Africa, South America, with smaller foci in Southeast Asia, South Africa, and northeastern Iran. HTLV-1 was initially isolated in 1980 from two T-cell lymphoblastoid cell lines and the blood of a patient originally thought to have a cutaneous T-cell lymphoma. It was the first human retrovirus ever associated with a human cancer. Three years before the isolation of HTLV-1, a Japanese group reported adult T-cell leukemia (ATL), a rare form of leukemia endemic to southwest Japan, as a distinct clinical entity. In 1981, the same group demonstrated that ATL was caused by a new human retrovirus originally termed 'ATLV'. Later, ATLV and HTLV have been shown to be identical, and a single name HTLV-1 has been adopted. In the mid-1980s, epidemiological data linked HTLV-1 infection with a chronic progressive neurological disease, which was termed 'tropical spastic paraparesis (TSP)' in the Caribbean and 'HTLV-1 associated myelopathy (HAM)' in Japan. HTLV-1-positive TSP and HAM were subsequently found to be clinically and pathologically identical and the disease was given a single designation as HAM/TSP. HTLV-1 can cause other chronic inflammatory diseases such as uveitis, arthropathy, pulmonary lymphocytic alveolitis, polymyositis, Sjögren syndrome, and infective dermatitis. Only approximately 2–3% of infected persons develop ATL and another 0.25–4% develop chronic inflammatory diseases, while the majority of infected individuals remain lifelong asymptomatic carriers (ACs). Thus, the viral, host, and environmental risk factors, as well as the host immune response against HTLV-1 infection, appear to regulate in the development of HTLV-1-associated diseases. For over two decades, the investigation of HTLV-1-mediated pathogenesis has focused on Tax, an HTLV-1-encoded viral oncoprotein. Tax activates many cellular genes by binding to groups of transcription factors and coactivators and is necessary and sufficient for cellular transformation. However, recent reports have identified another regulatory protein, HTLV-1 basic leucine zipper factor (HBZ), that plays a critical role in the development of ATL and HAM/TSP.

HTLV-1-Associated Diseases

Adult T-cell leukemia

ATL is a fatal malignancy of mature CD4+ T cells. It arises in only a small proportion of HTLV-1-infected people (1–5% of infected individuals) after long latency periods following primary infection. ATL shows diverse clinical features, but can be divided into four clinical subtypes: smoldering, chronic, lymphoma, and acute. Each subtype is directly correlated with the prognosis of patients: the smoldering and chronic types are indolent, while the acute and lymphoma types are aggressive and characterized by resistance to chemotherapy and poor prognosis. Development of ATL is characterized by infiltration of various tissues with circulating ATL cells, called 'flower cells', which have conspicuous lobulated nuclei. These cells cause further symptoms including lymphadenopathy, lytic bone lesions, skin involvement, hepatosplenomegaly, and hypercalcemia. Laboratory findings of ATL patients typically reveal a marked leukocytosis, hypercalcemia, high serum levels of lactate dehydrogenase (LDH), and a soluble form of interleukin-2 receptor (IL-2R). In cohort studies of HTLV-1 carriers, the risk factors for ATL appeared to include vertical infection (mother to child transmission), male gender, older age, and increasing numbers of abnormal lymphocytes. Since ATL occurs mainly in vertically infected individuals, but not in those who become infected later in life, the impairment of HTLV-1-specific T-cell responses caused by vertical HTLV-1 infection has been suggested as a possible cause of disease development. The HTLV-1-specific cytotoxic T-cell (CTL) responses from ATL patients are significantly lower than that of HAM/TSP patients. However, insufficient HTLV-1-specific T-cell responses might also occur during and after the onset of ATL. Although ATL has a poor prognosis, recent advances in its treatment have led to significant gains in response rates and

survival. Accumulating evidence suggests that allogeneic bone marrow transplantation and allogeneic peripheral blood stem cell transplantation are potent therapies for aggressive ATL (i.e., the acute and lymphoma type). The combination of the antiretroviral agent zidovudine (AZT) and interferon-alfa (IFN-α) is also beneficial for overall survival in smoldering and chronic (i.e., indolent) ATL, although its efficacy has not yet been confirmed in well-designed prospective studies.

Since the discovery of HTLV-1, the viral transactivator Tax has been viewed as critical for leukemogenesis, due to its pleiotropic effects on both viral and many cellular genes responsible for cell proliferation, genetic instability, dysregulation of the cell cycle, and apoptosis. However, Tax expression is not detected in about 60% of freshly isolated samples from ATL cases. Recently, the expression of another regulatory protein, HBZ, has been reported in association with all ATL cases. This protein, which is encoded in the minus or antisense strand of the virus genome, promotes proliferation of ATL cells and induces T-cell lymphomas in CD4+ T cells by transgenic expression, indicating involvement of HBZ expression in the development of ATL. In addition, among the HTLV-1-encoded viral genes, only the HBZ gene sequence remains intact, unaffected by nonsense mutations and deletion. Thus, HBZ expression is indispensable for proliferation and survival of ATL cells and HTLV-1-infected cells, and Tax expression is not always necessary for the development of ATL.

HTLV-1-Associated Myelopathy/Tropical Spastic Paraparesis

HAM/TSP is a chronic progressive myelopathy characterized by spastic paraparesis, sphincter dysfunction, and mild sensory disturbance in the lower extremities. In addition to neurological symptoms, some HAM/TSP cases also exhibit autoimmune-like disorders, such as uveitis, arthritis, T-lymphocyte alveolitis, polymyositis, and Sjögren syndrome. To date, more than 3000 cases of HAM/TSP have been reported in HTLV-1-endemic areas. Sporadic cases have also been described in nonendemic areas such as the United States and Europe, mainly in immigrants from an HTLV-1-endemic area. The lifetime risk of developing HAM/TSP is different among ethnic groups, ranging between 0.25% and 4%. The annual incidence of HAM/TSP is higher among Jamaican subjects than among Japanese subjects (20 vs. three cases/100 000 population), with a 2 to 3 times higher risk for women in both populations. The period from initial HTLV-1 infection to the onset of HAM/TSP is assumed to range from months to decades, a shorter time than for ATL onset. HAM/TSP occurs both in vertically infected individuals and in those who become infected later in life (i.e., through sexual contact (almost exclusively from male to female), intravenous drug use, contaminated blood transfusions, etc.). The mean age at onset is 43.8 years and, like other autoimmune diseases, the frequency of HAM/TSP is higher in women than in men (the male to female ratio of occurrence is 1:2.3).

The essential histopathological feature of HAM/TSP is a chronic progressive inflammation in the spinal cord, predominantly at the thoracic level. The loss of myelin sheaths and axons in the lateral, anterior, and posterior columns is associated with perivascular and parenchymal lymphocytic infiltration, reactive astrocytosis, and fibrillary gliosis. In addition to HTLV-1 antibody positivity, other laboratory findings of HAM/TSP include the presence of atypical lymphocytes (the so-called flower cells) in peripheral blood and cerebrospinal fluid (CSF), a moderate pleocytosis, and raised protein content in CSF. Oligoclonal bands, raised concentrations of inflammatory markers such as neopterin, tumor necrosis factor (TNF)-α, IL-6 and IFN-γ, and an increased intrathecal antibody synthesis specific for HTLV-1 antigens have also been described in CSF of HAM/TSP patients.

A previous population association study in HTLV-1 endemic in southwest Japan revealed that one of the major risk factors is the HTLV-1 proviral load (PVL), as the PVL is significantly higher in HAM/TSP patients than in ACs. A high PVL was also associated with an increased risk of progression to disease. Higher PVL in HAM/TSP patients than in ACs was also observed in other endemic areas such as the Caribbean, South America, and the Middle East. In southwest Japan, an association was suggested between possession of the HLA-class I genes HLA-A*02 and Cw*08 and a statistically significant reduction in both PVL and the risk of HAM/TSP. By contrast, possession of HLA-class I HLA-B*5401 and class II HLA-DRB1*0101 predisposed patients in the same population to HAM/TSP. Since the function of class I HLA proteins is to present antigenic peptides to CTL, these results imply that individuals with HLA-A*02 or HLA-Cw*08 mount a particularly efficient CTL response against HTLV-1, which may be an important determinant of HTLV-1 PVL and the risk of HAM/TSP.

To date, no generally agreed standard treatment regimen has been established for HAM/TSP, as no treatment for HAM/TSP has proven to be consistently effective and long term. Therefore, current clinical practice for treatment of HAM/TSP is based on case series and open, nonrandomized uncontrolled studies. Although mild to moderate beneficial effects have been reported with corticosteroids, immunosuppressants, high-dose intravenous gammaglobulin, antibiotics (erythromycin and fosfomycin), and vitamin C, the clinical benefits are only transient and limited. The complications of steroid use limit their use particularly in postmenopausal females, who are at higher risk of developing HAM/TSP. Only three randomized placebo-controlled trials have been conducted for HAM/TSP treatment. These studies indicate that IFN-α is an effective therapy, with an acceptable side-effects profile. By contrast, no evidence yet exists of any benefit of zidovudine plus lamivudine for treating HAM/TSP. More clinical trials with adequate power are needed in the future.

Other HTLV-1-Associated Diseases

HTLV-1 has been implicated in the pathogenesis of other inflammatory disorders such as uveitis, arthropathy, infective dermatitis, pulmonary lymphocytic alveolitis, polymyositis, Sjögren syndrome, and autoimmune thyroid diseases, based on the higher HTLV-1 PVL and the higher seroprevalence in patients than in ACs. However, direct evidence for an association between these disorders and HTLV-1 infection is still lacking. Nonetheless, HTLV-1 may be a significant trigger for the development of these autoimmune disorders.

See also: Retroviruses

Further Reading

Blattner WA (ed.) (1990) *Human Retrovirology: HTLV.* New York: Raven Press.

Höllsberg P and Hafler DA (eds.) (1996) *Human T-Cell Lymphotropic Virus Type I.* New York: Wiley.

Sugamura K, Uchiyama T, Matsuoka M, and Kannagi M (eds.) (2003) *Two Decades of Adult T-Cell Leukemia and HTLV-I Research: Gann Monograph on Cancer Research.* Tokyo: Japan Scientific Societies Press.

Saito *et al. Retrovirology* 2013, **10**:51
http://www.retrovirology.com/content/10/1/51

RETROVIROLOGY

RESEARCH Open Access

Increased expression of OX40 is associated with progressive disease in patients with HTLV-1-associated myelopathy/tropical spastic paraparesis

Mineki Saito[1,6*], Reiko Tanaka[1], Shiho Arishima[2], Toshio Matsuzaki[3], Satoshi Ishihara[4], Takashi Tokashiki[4], Yusuke Ohya[4], Hiroshi Takashima[3], Fujio Umehara[5], Shuji Izumo[2] and Yuetsu Tanaka[1]

Abstract

Background: OX40 is a member of the tumor necrosis factor receptor family that is expressed primarily on activated $CD4^+$ T cells and promotes the development of effector and memory T cells. Although OX40 has been reported to be a target gene of human T-cell leukemia virus type-1 (HTLV-1) viral transactivator Tax and is overexpressed *in vivo* in adult T-cell leukemia (ATL) cells, an association between OX40 and HTLV-1-associated inflammatory disorders, such as HTLV-1-associated myelopathy/tropical spastic paraparesis (HAM/TSP), has not yet been established. Moreover, because abrogation of OX40 signals ameliorates chronic inflammation in animal models of autoimmune disease, novel monoclonal antibodies against OX40 may offer a potential treatment for HTLV-1-associated diseases such as ATL and HAM/TSP.

Results: In this study, we showed that OX40 was specifically expressed in $CD4^+$ T cells naturally infected with HTLV-1 that have the potential to produce pro-inflammatory cytokines along with Tax expression. We also showed that OX40 was overexpressed in spinal cord infiltrating mononuclear cells in a clinically progressive HAM/TSP patient with a short duration of illness. The levels of the soluble form of OX40 (sOX40) in the cerebrospinal fluid (CSF) from chronic progressive HAM/TSP patients or from patients with other inflammatory neurological diseases (OINDs) were not different. In contrast, sOX40 levels in the CSF of rapidly progressing HAM/TSP patients were higher than those in the CSF from patients with OINDs, and these patients showed higher sOX40 levels in the CSF than in the plasma. When our newly produced monoclonal antibody against OX40 was added to peripheral blood mononuclear cells in culture, HTLV-1-infected T cells were specifically removed by a mechanism that depends on antibody-dependent cellular cytotoxicity.

Conclusions: Our study identified OX40 as a key molecule and biomarker for rapid progression of HAM/TSP. Furthermore, blocking OX40 may have potential in therapeutic intervention for HAM/TSP.

Keywords: HTLV-1, OX40, HAM/TSP, ADCC, Immunotherapy

* Correspondence: mineki@med.kawasaki-m.ac.jp
[1]Department of Immunology, Graduate School of Medicine, University of the Ryukyus, 207 Uehara, Okinawa 903-0215, Japan
[6]Present Address: Department of Microbiology, Kawasaki Medical School, 577 Matsushima, Kurashiki 701-0192, Japan
Full list of author information is available at the end of the article

Background

Human T-cell leukemia virus type 1 (HTLV-1) was the first human oncogenic retrovirus to be identified and associated with distinct human diseases such as adult T-cell leukemia (ATL) [1,2] and HTLV-1-associated myelopathy/tropical spastic paraparesis (HAM/TSP) [3,4]. HAM/TSP is a chronic progressive myelopathy characterized by spastic paraparesis, sphincter dysfunction, and mild sensory disturbance in the lower extremities [5]. In addition to neurological symptoms, some HAM/TSP patients also exhibit autoimmune-like disorders such as uveitis, arthritis, T-lymphocyte alveolitis, polymyositis, and Sjögren syndrome [6]. Major pathological features of HAM/TSP are chronic inflammation of the spinal cord, characterized by perivascular lymphocytic cuffing and parenchymal lymphocytic infiltration that includes HTLV-1-infected $CD4^+$ T cells [7]. In HAM/TSP patients, the median HTLV-1 proviral load (PVL), which reflects the *in vivo* number of HTLV-1-infected lymphocytes, is more than 10 times higher than that in asymptomatic carriers (ACs) [8]. An increase in PVL typically coincides with worsening of clinical symptoms [9]. Increased concentrations of inflammatory markers such as neopterin [10], tumor necrosis factor (TNF)-α, interleukin (IL)-6, and interferon (IFN)-γ [11], and increase in HTLV-1 antigen-specific intrathecal antibody synthesis [12] have been observed in the cerebrospinal fluid (CSF) of HAM/TSP patients. More recently, it has been reported that IFN-stimulated genes were overexpressed in circulating leukocytes and the expression correlated with the clinical severity of HAM/TSP [13]. These findings indicate that a pro-inflammatory environment, associated with increased numbers of HTLV-1-infected cells, is a characteristic immunologic profile of HAM/TSP.

OX40, also known as CD134 or TNFRSF4, is a member of the TNF co-stimulatory receptor family and is expressed on activated T cells [14]. OX40 is specifically up-regulated by the HTLV-1 viral transactivator Tax [15,16]. The ligand of OX40 (OX40L), which belongs to the TNF superfamily, was first identified as glycoprotein 34 (gp34) on HTLV-1-transformed cells [17], and it was later found to bind OX40 [18]. OX40-OX40L interactions alter the activity and differentiation of many kinds of immune cells, including regulatory T cells (Tregs), T cells, antigen-presenting cells (APCs), natural killer (NK) cells, and natural killer T (NKT) cells [14]. Previous studies have reported that OX40 is constitutively expressed in ATL cells and participate in cell adhesion [19]. Specifically, OX40 and OX40L directly mediate the adhesion of activated normal $CD4^+$ T cells, as well as HTLV-1-transformed T cells, to vascular endothelial cells [20]. Immunohistochemical staining of skin biopsy specimens from ATL patients also showed constitutive expression of OX40, suggesting its role in leukemic cell infiltration, in addition to *in vivo* cell adhesion [19].

Recent research has also shown the importance of OX40-OX40L interactions in the development of immune-mediated diseases. In particular, a strong reduction in disease severity or a complete lack of disease has been reported when OX40 or OX40L is absent or neutralized in animal models of multiple sclerosis (MS) [21], allergic asthma [22], colitis [23], diabetes [24], arthritis [25], atherosclerosis [26], graft versus host disease [27], and allograft rejection [28]. Although HTLV-1 causes an aggressive T cell malignancy (i.e., ATL) and chronic inflammatory diseases such as HAM/TSP, an association of OX40 with the inflammatory diseases observed in HTLV-1-infected individuals has not yet been established.

In this study, we investigated the expression of OX40 in HAM/TSP patients and found that the increased expression of OX40 is associated with the rapidly progressive disease. We also used an in-house monoclonal antibody (mAb) against human OX40 to test the potential of OX40 as a target molecule for immunotherapy.

Results

Tax-dependent constitutive expression of OX40 in HTLV-1-infected T cells

OX40 and OX40L have been reported to be overexpressed in HTLV-1-infected human T-cells lines [15,19,20]. These findings were obtained using northern blot or western blot analysis using whole cells; hence, our first aim was to confirm and extend these findings at the single-cell level using flow cytometry. Therefore, we used mAbs against human OX40 (clone B-7B5) and human OX40L (clone 5A8) produced in our laboratory. We analyzed six HTLV-1-infected human T-cell lines (HUT-102, MT-1, MT-2, MT-4, SLB-1, and C5/MJ). C5/MJ, SLB-1, and MT-4 cells have not been previously tested for OX40/OX40L expression. As shown in Figure 1A, expression levels were different in each cell line: OX40 was overexpressed on the surface of the Tax positive (Tax+) T-cell lines (HUT-102, MT-2, MT-4, SLB-1, and C5/MJ), but OX40 was not expressed on the surface of the Tax negative (Tax-) MT-1 cell line or the uninfected T cell line (CEM-OX40L). Consistent with previous studies, these findings suggested that OX40 expression is Tax dependent. In contrast, OX40L was not always expressed on the surface of HTLV-1-infected human T-cell lines or on the uninfected T cell line (CEM-OX40), irrespective of Tax expression (Figure 1B).

Next, we confirmed whether OX40 and OX40L protein expression on the cell surface is induced by Tax at the single-cell level by flow cytometry. We used JPX-9 cells [29], a Jurkat (HTLV-1 negative human T cell leukemia cell line) subclone generated by stable transfection of a functional Tax expression-plasmid vector, and induced Tax expression by adding $CdCl_2$ into the culture medium (final concentration: 10 μM). As shown in Figure 1C, treatment of JPX-9 cells with $CdCl_2$ induced expression of

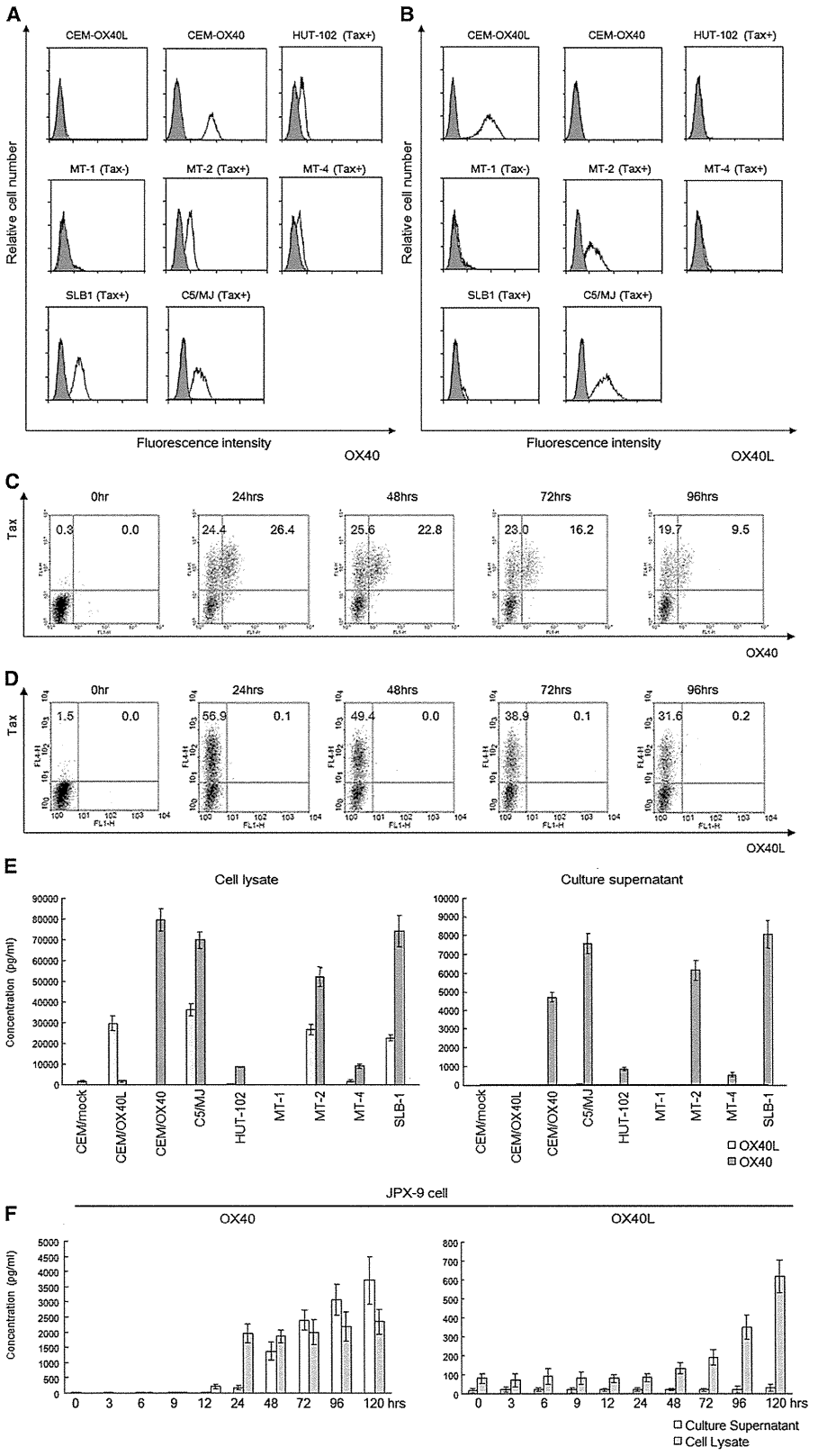

Figure 1 (See legend on next page.)

(See figure on previous page.)
Figure 1 Tax-dependent constitutive expression of OX40 in HTLV-1-infected T-cell lines and Tax-inducible JPX-9 cell line. **A.** Representative histograms of OX40 expression in 6 HTLV-1 infected T-cell lines (HUT-102, MT-1, MT-2, MT-4, C5/MJ, SLB-1) and two HTLV-1-uninfected T-cell lines (CEM-OX40L and CEM-OX40). Shaded histograms represent the isotype control. Tax+ or Tax- means whether these cells express Tax (Tax+) or not (Tax-). **B.** Representative histograms of OX40L expression in 6 HTLV-1 infected T-cell lines (HUT-102, MT-1, MT-2, MT-4, C5/MJ, SLB-1) and two HTLV-1-uninfected T-cell lines (CEM-OX40L and CEM-OX40). Shaded histograms are isotype controls. **C.** Flow cytometric analysis of expression of OX40 after induction of Tax in JPX-9 cells. **D.** Flow cytometric analysis of expression of OX40L after induction of Tax in JPX-9 cells. **E.** Soluble OX40 and OX40L levels in cell culture supernatant and cell lysate from 6 HTLV-1 infected T-cell lines (HUT-102, MT-1, MT-2, MT-4, C5/MJ, SLB-1) and three HTLV-1-uninfected T-cell lines (CEM-mock, CEM-OX40L and CEM-OX40). **F.** Soluble OX40 and OX40L levels in cell culture supernatant and cell lysate from JPX-9 cell line treated with $CdCl_2$ along with the induction of viral transactivator Tax.

Tax, and OX40 was expressed exclusively in cells that also expressed Tax. In contrast, OX40L was not expressed in JPX-9 cells even after 96 hours post Tax-induction (Figure 1D).

Previous reports indicated that the soluble forms of OX40 (sOX40) and OX40L (sOX40L) were detectable in serum of patients with autoimmune disease and cancer [30,31]. We therefore examined whether sOX40 and sOX40L levels were elevated in culture supernatants from HTLV-1 infected T-cell lines and JPX-9 cells before and after induction of Tax. In agreement with our flow cytometry data (Figure 1A), sOX40 was detected in both culture supernatants and cell lysates of Tax positive C5/MJ, HUT102, MT-2, MT-4, and SLB-1 cells (Figure 1E, gray bar). However, sOX40L was not detected in culture supernatants of any of the samples tested, but it was readily detectable in cell lysates of Tax positive C5/MJ, MT-2, MT-4 and SLB1 cells (Figure 1E, light gray bar). We next examined whether soluble OX40 and OX40L are induced by Tax in JPX-9 cells. Addition of $CdCl_2$ to the culture medium of JPX-9 cells resulted in a concomitant increase in sOX40 expression within 24 hours, indicating a strong correlation and functional link between Tax and sOX40 expression (Figure 1F, left panel). Interestingly, although OX40L was already present before induction of Tax, OX40L expression was increased after 24 hours but was never released into the culture supernatant as sOX40L within 120 hours after induction of Tax (Figure 1F, right panel).

Functional OX40 is specifically expressed on the surface of T cells naturally infected with HTLV-1 that have the potential to produce pro-inflammatory cytokines

Next, we tested whether OX40 or OX40L expression is also activated in naturally infected T cells isolated directly from HTLV-1-infected individuals. PBMCs were collected from three non-infected controls (NCs), three ACs, and four HAM/TSP patients. PBMCs were isolated from blood samples and harvested directly, or after a 16-hour in vitro cultivation in the absence of any growth factors or mitogens. After harvesting, cell samples were fixed and processed for concomitant detection of Tax, OX40, or OX40L, and CD4 expression by flow cytometry. Similar to the findings for JPX-9 cells, OX40 was detected with an anti-OX40 mAb (clones B-7B5) after 16 hours of in vitro cultivation (Figure 2A), but OX40L was not detected in cultured PBMCs from a HAM/TSP patient (HAM/TSP1) (Figure 2B). Figure 2C shows that the Tax protein was detected in $CD4^+$ T cells after cultivation. Similar to the JPX-9 cell experiments, OX40 was expressed almost exclusively in the naturally infected $CD4^+$ T cells that also expressed Tax (Figure 2D). Similar findings were observed in all samples tested, irrespective of disease status (i.e., HAM/TSP or ACs) (Additional file 1: Figure S1 and Additional file 2: Table S1). The cells from NCs did not express either OX40 or Tax in $CD4^+$ T cells, before or after cultivation (data not shown). Real time RT-PCR also showed that mRNA expression of HTLV-1 tax and OX40 in $CD4^+$ T cells was increased after cultivation, both in HAM/TSP patients and ACs (Figure 2E).

It has recently been reported [32], that the expression of another co-stimulatory member of the TNFR family, 4-1BB, is also up-regulated ex vivo in $CD4^+$ T cells from HTLV-1-infected individuals, and it was found to be correlated with Tax expression (Additional file 1: Figure S2A and B). However, the expression of OX40 is more specific for Tax^+CD4^+ cells than 4-1BB (Figure 2D and Additional file 1: Figure S2C).

Next, we sought to determine if OX40, expressed on the surface of Tax^+CD4^+ T cells from HTLV-1-infected individuals, is functional. We incubated aliquots of Fc-blocked PBMCs with biotinylated recombinant soluble OX40L at a concentration of 2.5 mg/ml for 30 min on ice. Cells were then fixed and processed for concomitant detection of Tax, CD4, and PE-streptavidin by flow cytometry. As shown in Additional file 1: Figure S3, the frequency of $CD4^+$ T cells that were positively stained with biotinylated recombinant soluble OX40L and PE-streptavidin was similar to the percentage of $CD4^+$ T cells stained by anti-OX40 mAb, indicating that these cells expressed functional OX40.

We further analyzed if $CD4^+OX40^+$ T cells in HAM/TSP patients were capable of producing the inflammatory and neurotoxic cytokines, IFN-γ and TNF-α, which, according to the bystander damage hypothesis, could cause central nervous system (CNS) inflammation and demyelination seen in HAM/TSP patients [33,34]. The frequency of pro-inflammatory cytokine positive cells within the $OX40^+CD4^+$ and Tax^+CD4^+ populations from

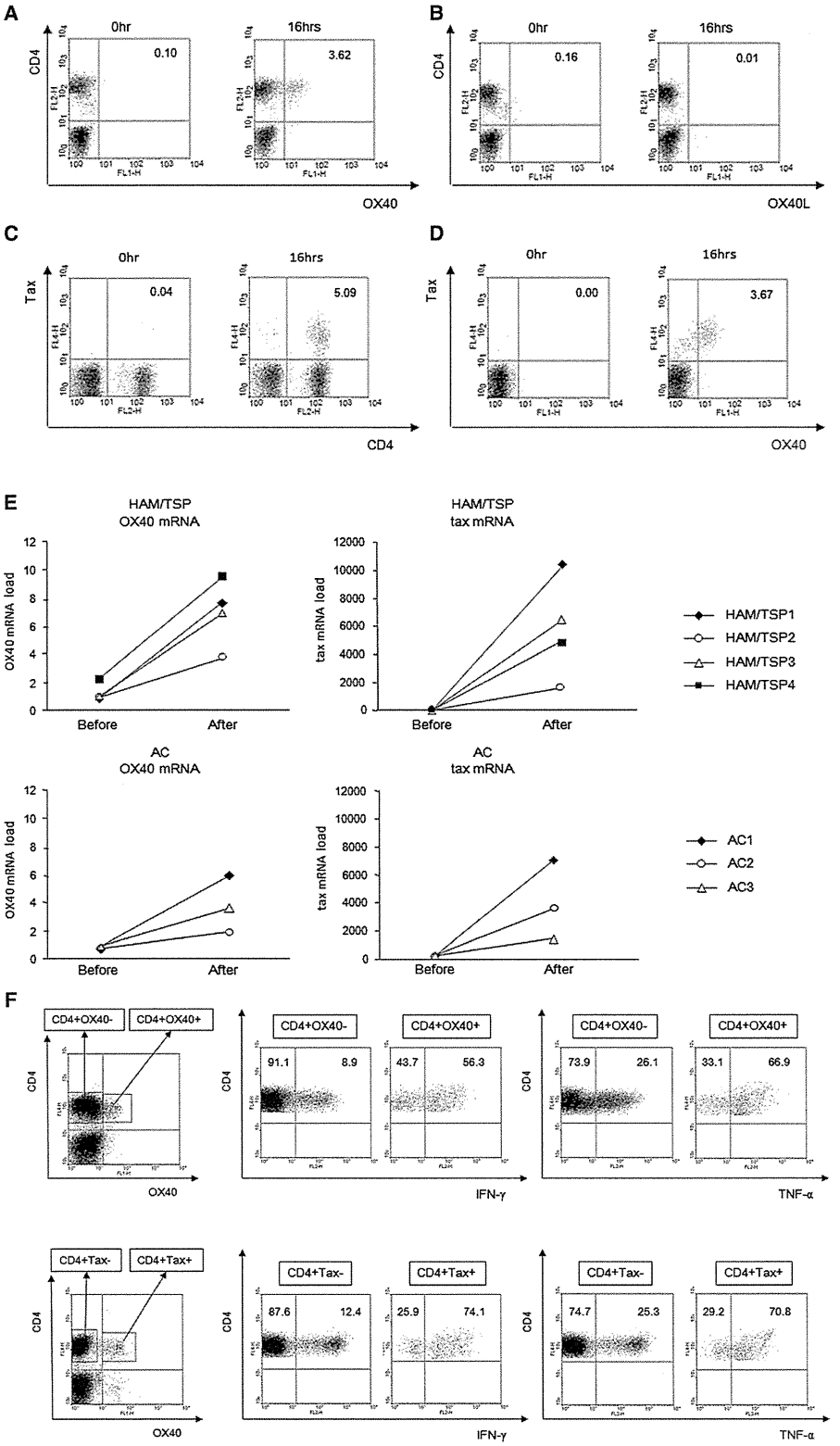

Figure 2 (See legend on next page.)

(See figure on previous page.)
Figure 2 OX40 is specifically expressed on the surface of T cells naturally infected with HTLV-1 that have the potential to produce pro-inflammatory cytokines. A. OX40 was detected on $CD4^+$ T cells of HAM/TSP patient with anti-OX40 mAb (clones B-7B5) after 16 hours *in vitro* cultivation in the absence of any growth factors or mitogen. **B.** OX40L was not detected on $CD4^+$ T cells of HAM/TSP patient with anti-OX40L mAb (clones 5A8) after 16 hours *in vitro* cultivation in the absence of any growth factors or mitogen. **C.** Tax protein was detected in $CD4^+$ T cells of HAM/TSP patient after 16 hours *in vitro* cultivation. **D.** OX40 was expressed almost exclusively in naturally infected $CD4^+$ T cells that also expressed Tax in HAM/TSP patient. **E.** Both HTLV-1 tax and OX40 mRNA expression in $CD4^+$ T cells was increased after 16 hours *in vitro* cultivation. **F.** The frequency of pro-inflammatory cytokine positive cells within the $OX40^+CD4^+$ and Tax^+CD4^+ populations from HTLV-1 infected individuals are significantly higher than $OX40^-CD4^+$ and Tax^-CD4^+ T cells, respectively ($p<0.001$, Student's t- test). One representative experiment of HAM/TSP patient (HAM/TSP1) is shown.

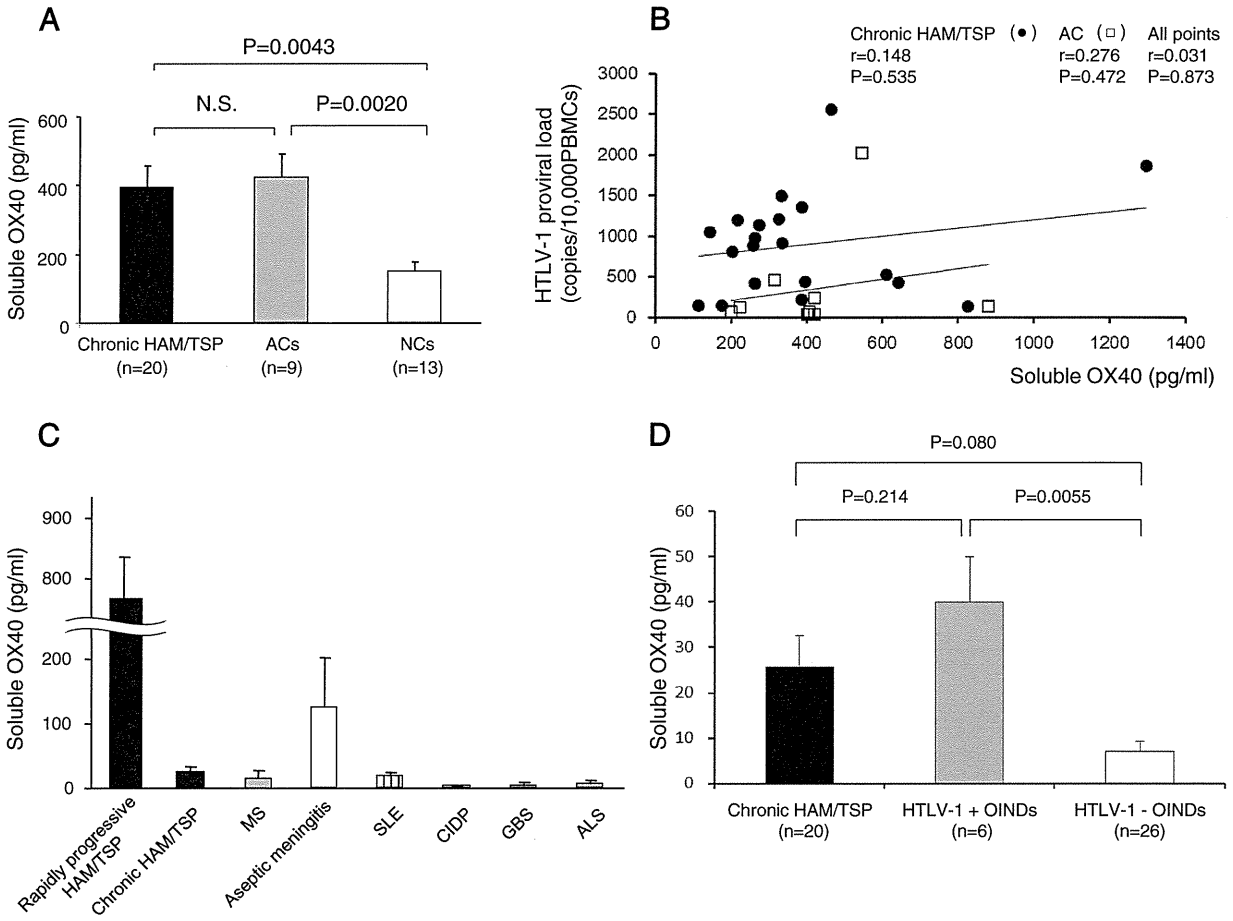

Figure 3 Increased expression of OX40 in vivo in rapidly progressive HAM/TSP patients. A. The plasma levels of soluble OX40 (sOX40) measured by ELISA. The plasma levels of sOX40 in typical HAM/TSP patients (chronic HAM: n=20), asymptomatic carriers (ACs: n=9) and normal uninfected healthy controls (NCs: n=13). **B.** No correlation between the plasma levels of sOX40 and HTLV-1 proviral load (tax copies/10,000PBMCs) from 29 HTLV-1 infected individuals (20 chronic HAM/TSP patients and 9 ACs). Data were analyzed by Spearman rank correlation. **C.** The cerebrospinal fluid (CSF) levels of sOX40 in rapidly progressive HAM/TSP patients (n=3), chronic HAM/TSP patients (n=22) and other neurological diseases including multiple sclerosis (MS) (n=12), aseptic meningitis (n=8), systemic lupus erythematosus (SLE) with neurological manifestations (n=5), chronic inflammatory demyelinating polyneuropathy (CIDP) (n=9), Guillain-Barré syndrome (GBS) (n=6), and amyotrophic lateral sclerosis (ALS) (n=9). Chronic HAM/TSP means typical cases fulfilling diagnostic criteria and rapidly progressive HAM/TSP is defined by patients' incapacity to walk unaided within three months after symptoms' onset. **D.** The levels of sOX40 in the CSF from HTLV-1 infected other inflammatory neurological diseases (HTLV-1+ OINDs), i.e. any inflammatory neurological disorders except for HAM/TSP which occurred in HTLV-1 infected individuals, was not significantly different from that of chronic HAM/TSP, whereas the levels of sOX40 from HTLV-1+ OINDs was significantly increased than that of non-infected OINDs (HTLV-1- OINDs). HTLV-1+ OINDs: 1 multiple sclerosis (MS), 1 SLE with neurological manifestations, 4 aseptic meningitis. HTLV-1- OINDs: 9 MS, 5 SLE with neurological manifestations, 7 CIDP, 5 GBS.